Laboratori Nazionali di Frascati

LNF-92/023 (P)
8 Aprile 1992

G. Colangelo, S. Dubnička, M. Greco

RADIATIVE CORRECTIONS AT DAΦNE

Contribution to the DAΦNE Physics Handbook

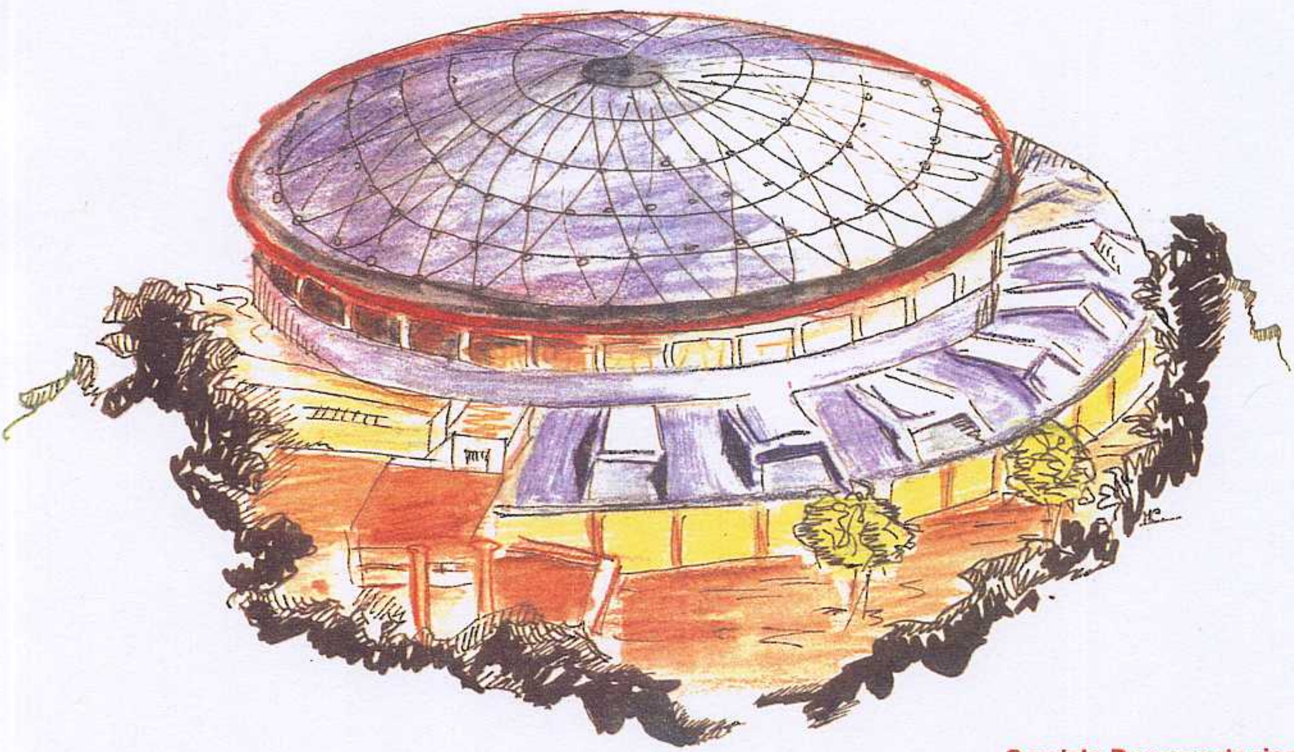

Servizio Documentazione
dei Laboratori Nazionali di Frascati
P.O. Box, 13 - 00044 Frascati (Italy)

INFN - Laboratori Nazionali di Frascati
Servizio Documentazione

LNF-92/023 (P)
8 Aprile 1992

Radiative Corrections at DAΦNE

G. Colangelo

INFN, Laboratori Nazionali di Frascati, I-00044, Frascati, Italy

S. Dubnička

Joint Institute for Nuclear Research, Dubna, Russia

M. Greco

Dipartimento di Fisica Nucleare e Teorica dell'Universita', I-27100, Pavia, Italy

and INFN, Laboratori Nazionali di Frascati, I-00044, Frascati, Italy

ABSTRACT

The status of QED radiative corrections in the vicinity of the ϕ is summarized for leptonic and $\pi^+\pi^-$, K^+K^-, $K^0,\overline{K}^0$ final states. Simple analytical formulae are given of immediate phenomenological application. A few numerical examples are also given explicitly.

The important role played by e.m. radiative corrections in the production of narrow states in e+ e- annihilation is well known [1]. A general non perturbative approach has been introduced [2] in connection with the production of the J/ψ, which takes into account the large double and single soft and collinear logarithms of perturbation theory to all orders, the remaining terms being exactly calculated to one loop accuracy. This approach leads to a level of precision of order of 1%. The necessity of testing the electroweak theory at LEP beyond the tree level to an accuracy of better than 1%, has led to further improve the theoretical accuracy with explicit two-loop calculations[3-4]. Those have been performed for the Z line shape, the production of μ pairs and Bhabha scattering.

The simple application of those results to ϕ production gives in a straightforward manner a very accurate description of the e.m. effects occurring at DAΦNE, with the appropriate changes of the masses, widths and coupling constants. In particular the main radiative factor $\beta_e = 2\alpha/\pi(L_e - 1)$, with $L_e = \ln(s/m_e^2)$, takes the value $\beta_e = 0.066$ at $s = M_\phi^2$, instead of $\beta_e = 0.11$ for $s = M_Z^2$. On the other hand the infrared logarithm $\ln(M/\Gamma)$ takes a larger value in the case of the ϕ, namely $\ln(M_\phi/\Gamma_\phi) = 5.44$ to be compared to $\ln(M_Z/\Gamma_Z) = 3.57$. Therefore the effect of the radiative corrections at $s = M_\phi^2$, of order $(\Gamma_\phi/M_\phi)^{\beta_e} = 0.7$, leads to an important reduction of the peak cross section and other sizeable effects relevant for the determination of the observable quantities.

The aim of the present work is to summarize the status of e. m. effects at DAΦNE, giving in addition simple formulae of immediate phenomenological application. We consider the infrared factors to all orders, the left over terms of order α and leading order α^2 being explicitly reported for the main processes of experimental interest. We first consider a fermionic final state $f\bar{f}$ ($f \neq e$), with the line shape as a particular case, then Bhabha scattering, and finally $\pi^+\pi^-$ and K^+K^- pairs. A few numerical examples are given explicitly.

The Born cross sections for the pure QED, interference and resonant terms corresponding to the s-channel process $e^+e^- \to f\bar{f}$ ($f = \mu, q, .. \neq e$) are:

$$\frac{d\sigma_0^{QED}}{d\Omega} = \frac{\alpha^2}{4s} Q_f (1 + z^2)$$

$$\frac{d\sigma_0^{INT}}{d\Omega} = \frac{\alpha^2}{4s} (-Q_f)(1 + z^2)\, r_v\, [2\, \mathrm{Re}\, \chi(s)] \tag{1}$$

$$\frac{d\sigma_0^{RES}}{d\Omega} = \frac{\alpha^2}{4s} (1 + z^2)\, r_v^2\, |\chi(s)|^2$$

where $z = \cos\theta$, corresponding to a pure vector coupling of the ϕ to both e^+e^- and $f\bar{f}$, and Q_f being the fermion electric charge ($Q_f = -1$ for $f=\mu$), $r_v = (v_f/v_e)$ and

$$\Gamma(\phi \rightarrow f\bar{f}) = \frac{1}{3}\alpha\, v_f^2\, M_\phi$$

$$\chi(s) = v_e^2 \frac{s}{s - M_\phi^2 + iM_\phi\Gamma_\phi} \tag{2}$$

Initial state radiation effects can be simply described in the approach of structure functions by the basic formula [5] ($\varepsilon = \Delta E/E$)

$$\sigma(s) = \int_0^\varepsilon dx\, \sigma_0[(1 - x)s]\, H_e(x,s), \tag{3}$$

where the electron "radiator" function $H_e(x,s)$ takes into account the effect of the soft radiation to all orders and of the hard one up to $o(\alpha^2)$ as[6]

$$H_e(x,s) = \Delta_e(s)\, \beta_e\, x^{\beta_e - 1} - \frac{1}{2}\beta_e (2 - x) + \frac{1}{8}\beta_e^2 \left\{(2 - x)\,[\,3 \ln(1-x) - 4 \ln x] - \frac{4}{x}[\ln(1-x)] + x - 6\right\}, \tag{4}$$

with

$$\Delta_e(s) = 1 + \frac{\alpha}{\pi}\left[\frac{3}{2} L_e + 2\,(\zeta(2) - 1)\right] + \left(\frac{\alpha}{\pi}\right)^2$$

$$\left\{\left[\frac{9}{8} - 2\,\zeta(2)\right] L_e^2 + \left[3\,\zeta(3) + \frac{11}{2}\,\zeta(2) - \frac{45}{16}\right] L_e + \right.$$

$$\left.\left[-\frac{6}{5}\,\zeta^2(2) - \frac{9}{2}\,\zeta(3) - 6\,\zeta(2)\ln 2 + \frac{3}{8}\,\zeta(2) + \frac{57}{12}\right]\right\}$$

$$\equiv 1 + \left(\frac{\alpha}{\pi}\right)\ \Delta_e^{(1)} + \left(\frac{\alpha}{\pi}\right)^2 \Delta_e^{(2)} \qquad (5)$$

When the energy resolution is small (ε<<1), as it will be the case for most experiments at DAΦNE, then eq. (3) is valid with very good approximation also at the level of differential cross sections. Furthermore it can be analitically solved[7] after inserting the Born cross sections (1), and the final result can be cast in the form[8]

$$\frac{d\sigma}{d\Omega} = \sum_i \frac{d\sigma^{(i)}}{d\Omega} \left\{C^{(i)}_{infra}\left[1 + \overline{C}^{(i)}_F\right] + C^{(i)}_H + C'^{(i)}_F\right\}, \qquad (6)$$

with i = QED, INT, RES and

$$C^{QED}_{infra} = \varepsilon^{\,\beta_e + \beta_f + 2\,\beta_{int}}$$

$$C^{INT}_{infra} = \frac{\varepsilon^{\,\beta_f + \beta_{int}}}{\cos\delta_R}\,\mathrm{Re}\left\{e^{i\delta_R}\left[\frac{\varepsilon}{1 + \frac{\varepsilon s}{M\Gamma}\sin\delta_R\exp(i\delta_R)}\right]^{\beta_e}\left[\frac{\varepsilon}{\varepsilon + \frac{M\Gamma}{s}\frac{\exp(-i\delta_R)}{\sin\delta_R}}\right]^{\beta_{int}}\right\} \qquad (7)$$

$$C^{RES}_{infra} = \varepsilon^{\,\beta_f}\left|\frac{\varepsilon}{1 + \frac{\varepsilon s}{M\Gamma}\sin\delta_R\exp(i\delta_R)}\right|^{\beta_e}\left|\frac{\varepsilon}{\varepsilon + \frac{M\Gamma}{s}\frac{\exp(-i\delta_R)}{\sin\delta_R}}\right|^{2\beta_{int}}[\cos\beta_e\phi - \mathrm{ctg}\delta_R\,\sin\beta_e\phi]$$

where $\beta_f = 2\alpha/\pi\ Q_f^2[\ln(s/m_f^2)-1]$, $\beta_{int} = -\,4\alpha/\pi\ Q_f\ln(\mathrm{tg}\theta/2)$, $\delta_R = \delta_R(s)$ and $\phi = \phi(s,\varepsilon)$ are defined as:

$$\frac{s}{M_R^2 - s} \equiv \frac{s}{M\Gamma} \sin\delta_R(s) \exp[i\delta_R(s)]$$

$$\phi = \text{arctg}\,\frac{\varepsilon s + M^2 - s}{M\Gamma(1 - \varepsilon)} - \text{arctg}\,\frac{M^2 - s}{M\Gamma} \qquad (8)$$

and $\Gamma = \Gamma(s) = \Gamma(M^2)(s/M^2)$. The factors $C_H^{(i)}$ take into account initial state hard photon radiation and have a leading logarithmic behaviour. The angular dependence coming from the box diagrams and bremsstrahlung terms is included in the factors $C'^{(i)}_F$. A detailed discussion of the various factors $\overline{C}^{(i)}_F$, $C_H^{(i)}$, $C'^{(i)}_F$ is given in the Appendix.

The above eqs.(6) include the emission from the final state and initial-final states interference terms, in addition to the pure initial state effects of eq. (1). More explicitly they take into account soft and hard bremsstrahlung, vertex corrections and (γ,γ) and (γ,ϕ) box diagrams. The real part of the vacuum polarization function $\delta_{VP}(s)$ can be absorbed, to all orders, into the definition of the e.m. running coupling constant, namely $e^2(1 + \text{Re}\delta_{VP}(s) + ...) = e^2/(1-\text{Re}\delta_{VP}(s)) = e^2(s)$ in the Born amplitude.

The result for the ϕ line shape can be simply obtained from the above equations by considering a neutral final state, namely by taking $\beta_f = \beta_{int} = 0$ in eq. (7) and similarly for the factors $\overline{C}^{(i)}_F$, $C_H^{(i)}$, $C'^{(i)}_F$ in eq. (6).

For the process of Bhabha scattering the Born cross sections (1) have to be extended to include the effect of the t-channel γ exchange. Then, using the notation of ref.[9], the various lowest order cross sections are defined as follows:

$$d\sigma_o\,(1) \equiv d\sigma_o\,[\gamma(s), \gamma(s)] = \frac{\alpha^2}{4s}\,(1 + z^2)$$

$$d\sigma_0\,(2) \equiv d\sigma_0\,[\gamma(s),\,\gamma(t)] = -\,\frac{\alpha^2}{4s}\,\frac{2\,(1+z)^2}{1-z}$$

$$d\sigma_0\,(3) \equiv d\sigma_0\,[\gamma(t),\,\gamma(t)] = \frac{\alpha^2}{4s}\,\frac{2}{(1-z)^2}\,[\,(1+z)^2+4]$$

$$d\sigma_0\,(7) \equiv d\sigma_0\,[\phi(s),\,\gamma(s)] = \frac{\alpha^2}{4s}\,(\,1+z^2)\;\;r_v\,[2\,\mathrm{Re}\,\chi(s)\,] \qquad (9)$$

$$d\sigma_0\,(8) \equiv d\sigma_0\,[\phi(s),\,\gamma(t)] = -\,\frac{\alpha^2}{4s}\,\frac{(1+z)^2}{1-z}\,[2\,\mathrm{Re}\,\chi(s)\,]$$

$$d\sigma_0\,(10) \equiv d\sigma_0\,[\phi(s),\,\phi(s)] = \frac{\alpha^2}{4s}\,(\,1+z^2)\;\;|\,\chi(s)|^2$$

Comparing with the similar expressions for the electroweak case with γ and Z exchanges, it is obvious that the terms corresponding to the ϕ exchange in the t-channel, i.e. $d\sigma_0$ (i), with i = 4,5,6,9, are missing. As in the case of μ pairs production, radiative corrections to Bhabha scattering have been performed[4] up to two-loop accuracy in the vicinity of the Z. Then, in analogy to eq, (6), and in the limit of small energy resolution one obtains from ref. [8]

$$\frac{d\sigma}{d\Omega} = \Sigma_i\,\frac{d\sigma^{(i)}}{d\Omega}\,\left\{C^{(i)}_{\mathrm{infra}}\left[1+\overline{C}^{(i)}_{F}\right]+C^{(i)}_{H}+C'^{(i)}_{F}\right\} \qquad (10)$$

where i=1,2,3,7,8 and 10. The infrared factors are obtained from eq. (7) as $C^{(i)}_{\mathrm{infra}} = C^{\mathrm{QED}}_{\mathrm{infra}}$ (i=1,2,3), $C^{(i)}_{\mathrm{infra}} = C^{\mathrm{INT}}_{\mathrm{infra}}$ (i=7,8) and $C^{(10)}_{\mathrm{infra}} = C^{\mathrm{RES}}_{\mathrm{infra}}$ with the substitution $\beta_f = \beta_e$. The leftover factors are given in the Appendix.

The radiative corrections to $\pi^+\pi^-$ and K^+K^- production can be simply performed by using eq. (3) with the help of an appropriate description of the π and K form factors. In the following we will use the model of ref.[10], which includes ρ, ω and ϕ exchanges, as well as the appropriate recurrences of those vector mesons, in a general framework which is consistent with unitarity and in accord with all experimental data in the space- and time-like regions.The implications of this model in the time-like region are shown in Figs. (1-2).

We perform now some numerical studies to illustrate the effect of the radiative corrections. The energy resolution is assumed to be ε=0.01 or ε=0.05. In the case of μ-pair production or Bhabha scattering, the final leptons are integrated over the polar angle θ, with $43^o \leq \theta \leq 137^o$. In Fig. 3 we show the ϕ line-shape for ε=0.01.

We plot the μ-pair production cross section in Figs. (4-5), and the Bhabha cross sections in Figs. (6-7), for $\varepsilon = 0.02$ and $\varepsilon = 0.08$; the angle δ is defined below.

For the case of $\pi^+\pi^-$ production Figs. (8a-8b) show the absolute and relative effect of the radiative corrections for ε=0.01, while in Figs. (9a-9b) ε is varied to ε=0.05. Similarly the charged K cross sections are shown in Figs. (10a-10b) for ε=0.01 and in Figs. (11a-11b) for $\varepsilon = 0.05$. Finally the $K^o, \overline{K}^o$ case is reported in Figs. (12a-12b) for ε=0.01.

The production of hard photons at large angles, particularly in a leptonic final state, will be discussed elsewhere. On the other hand, when the hard photon is emitted collinearly to the final particles within a small cone of angle δ (see figs. (4-7)), the appropriate modification of eqs. (6) and (10) is straightforward, as discussed in detail in the case of the Z production at LEP [1].

To conclude we have presented the general formalism for taking into account electromagnetic radiative effects in the vicinity of the ϕ at DAΦNE as well as numerical applications for most common reactions of experimental interest.

Appendix

We report below the explicit expression of the factors $\overline{C}_F^{(i)}$, $C_H^{(i)}$, $C'^{(i)}$ appearing in eqs. (6) and (10). A more detailed discussion as well as the derivation of the formulae below can be found in the original papers.

For the reaction $e^+e^- \to f\bar{f}$ we have:

$$\overline{C}_F^{QED} = \frac{\alpha}{\pi}[\Delta_e^{(1)} + \Delta_f^{(1)}] - \varepsilon(\beta_f - \beta_e) + \left(\frac{\alpha}{\pi}\right)^2 [\Delta_e^{(2)} + \Delta_f^{(2)} + \Delta_f^{(1)}\Delta_e^{(1)}] - \frac{\pi^2}{6}\overline{\beta}_f\,\overline{\beta}_e$$

$$\overline{C}_F^{INT} = \frac{\alpha}{\pi}[\Delta_e^{(1)} + \Delta_f^{(1)}] - \varepsilon\beta_f + \left(\frac{\alpha}{\pi}\right)^2 [\Delta_e^{(2)} + \Delta_f^{(2)} + \Delta_f^{(1)}\Delta_e^{(1)}]$$
$$- \frac{\pi^2}{6}\overline{\beta}_f\,\overline{\beta}_e \qquad \text{(A1)}$$

$$\overline{C}_F^{RES} = \frac{\alpha}{\pi}[\Delta_e^{(1)} + \Delta_f^{(1)}] - \varepsilon\beta_f + \left(\frac{\alpha}{\pi}\right)^2 [\Delta_e^{(2)} + \Delta_f^{(2)} + \Delta_f^{(1)}\Delta_e^{(1)}] - \frac{\pi^2}{6}\beta_f\,\bar{\bar{\beta}}_e$$

with $\overline{\beta}_{e,f} = \beta_{e,f} + \beta_{int}$, $\bar{\bar{\beta}}_e = \beta_e + 2\,\beta_{int}$, and $\Delta_f^{(1,2)}$ are trivially obtained from $\Delta_e^{(1,2)}$ with e->f. Furthermore the hard terms coming from initial state radiation are:

$$C_H^{QED} = -\varepsilon^{\overline{\beta}_f}(\beta_e\varepsilon)\left(1 + \frac{1}{4}\overline{\beta}_e\right)$$

$$C_H^{INT} = \varepsilon^{\overline{\beta}_f}\frac{(s-M^2)^2 + M^2\Gamma^2}{s(s-M^2)}\overline{\beta}_e\left(1 + \frac{1}{4}\overline{\beta}_e\right)\frac{1}{1+\gamma^2}[\ln|1 - z| + \phi\gamma] \qquad \text{(A2)}$$

$$C_H^{RES} = -\varepsilon^{\beta_f}\frac{(s-M^2)^2 + M^2\Gamma^2}{s^2}\bar{\bar{\beta}}_e\left(1 + \frac{1}{4}\beta_e\right)\frac{1}{\gamma(1+\gamma^2)}[\phi - \gamma\ln|1 - z|]$$

where $\gamma = \Gamma(M^2)/M$ and $z = \varepsilon\dfrac{1 + i\gamma}{s - M_R^2}$. Finally the expression of the factors $C'^{(i)}$, which essentially contain the angular dependence coming from bremsstrahlung and box diagrams, is too long to be reported here and can simply be obtained from ref. [1].

In the case of Bhabha scattering one obtains very similar results. However, whereas the factors $C_H^{(i)}$ in eq. (10) are simply obtained from (A2) for $\beta_f = \beta_e$, the factors $\overline{C}_F^{(i)}$ take a much more involved form due to the t-channel exchange. They are explicitly given in ref. [8] and will not be reported here again. Similarly the factors $C'^{(i)}$ can be easily obtained from ref. [4].

References

[1] For a review see for example, M. Greco, La Rivista del Nuovo Cimento 11, n. 5 (1988).

[2] G. Pancheri, Il Nuovo Cimento 60 A, 321 (1969), M. Greco, G. Pancheri and Y. Srivastava, Nucl. Phys. B101, 234 (1975) and 171, 118 (1980).

[3] F.A. Berends, W.L. Van Neerven and G.J.H. Burgers, Nucl. Phys. B 297, 429 (1988),

O. Nicrosini and L. Trentadue, Z. Phys. C 39, 479 (1988).

[4] F. Aversa, M. Greco, G. Montagna and O. Nicrosini, Phys. Lett. B 247, 93 (1990).

[5] E.A. Kuraev and V.S. Fadin, Sov. J. Nucl. Phys. 41, 466 (1985).

[6] O. Nicrosini and L. Trentadue, Phys. Lett. B 196, 551 (1987).

[7] F. Aversa and M. Greco, Phys. Lett. B 228, 134 (1989).

[8] F. Aversa and M. Greco, Phys. Lett. B 271, 435 (1991).

[9] M. Consoli, S. Lo Presti and M. Greco, Phys. Lett. B 113, 415 (1982); M. Greco, Phys. Lett. B 177, 97 (1986).

[10] S. Dubnicka, Nuovo Cimento 100 A, 1 (1988); M.E. Biagini, S. Dubnicka, E. Etim, and P. Kolar, Nuovo Cimento 104 A, 363 (1991).

Figure captions

Fig. 1	π form factor calculated according to ref. [10] fitted to all the experimental data available.
Fig. 2	K form factor calculated according to ref. [10] fitted to all the experimental data available.
Fig. 3	ϕ line-shape. Solid = Born cross section; dashed = Born + exponentiation + 1st order finite corrections; dotted = Born + exponentiation + 1st and 2nd order finite corrections.
Figs. 4-5	μ-pair production cross section.
4a	Only σ^{QED}: solid = Born cross section; dashed = Born + exponentiation + 1st order finite corrections; dotted = Born + exponentiation + 1st and 2nd order finite corrections. ($\delta = 5^o$)
4b	Solid = σ^{QED} completely corrected; dashed = solid + σ^{INT} at the born level; dotted = dashed + σ^{RES} at the Born level. ($\delta = 5^o$)
4c	Solid = σ^{QED} completely corrected + σ^{INT} + σ^{RES} at the Born level; dashed = $\sigma^{QED}+\sigma^{INT}+\sigma^{RES}$ completely corrected. ($\delta = 5^o$)
5	This figure shows the effect of the variation of δ to $\sigma^{QED}+\sigma^{INT}+\sigma^{RES}$ completely corrected: solid = ($\delta = 5^o$); dashed = ($\delta = 10^o$).
Figs. 6-7	Bhabha scattering cross section.
6a	QED contributions completely corrected. Dashed = $\sigma(1)$; solid = $\sigma(2)$; dotted = $\sigma(3)$; dotdashed = $\sigma(1)+\sigma(2)+\sigma(3)$.
6b	Effect of 2nd order finite corrections to $\sigma(1)+\sigma(2)+\sigma(3)$: solid = with; dashed = without.
6c	Effect of the variation of δ on $\sigma(1)+\sigma(2)+\sigma(3)$: solid = ($\delta = 10^o$); dashed = ($\delta = 5^o$).

7 In this figure we compare the effect of ϕ exchange to 2^{nd} order QED finite corrections (for $\delta = 5^{o}$):

solid = $\sigma(1)+\sigma(2)+\sigma(3)$ without 2^{nd} order;

dashed = $\sigma(1)+\sigma(2)+\sigma(3)$ with 2^{nd} order;

dotted = same as dashed + $\sigma(7)+\sigma(8)+\sigma(10)$ at the Born level;

dotdashed = same as dashed + $\sigma(7)+\sigma(8)+\sigma(10)$ completely corrected.

Fig. 8 Charged π's production cross section. Effect of QED radiative corrections for $\varepsilon = 0.01$.

Fig. 9 Same as before for $\varepsilon = 0.05$.

Fig. 10 Charged K's production cross section. Effect of QED radiative corrections for $\varepsilon = 0.01$.

Fig. 11 Same as before for $\varepsilon = 0.05$.

Fig. 12 Neutral K's production cross section. Effect of QED radiative corrections for $\varepsilon = 0.01$.

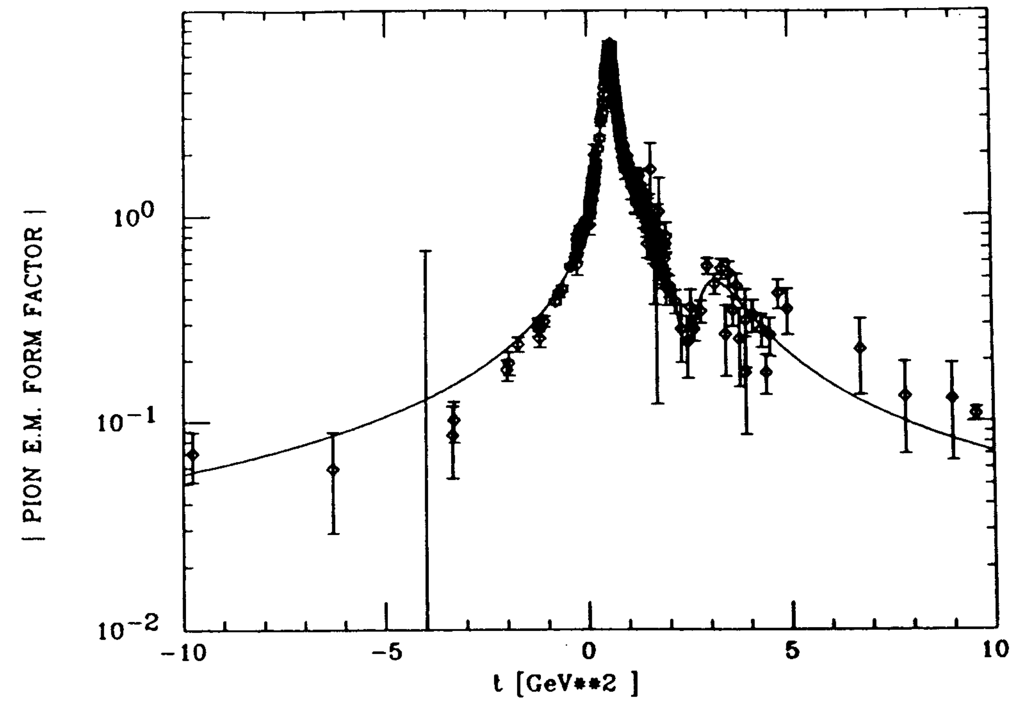
| PION E.M. FORM FACTOR |
10^0
10^{-1}
10^{-2}
-10
-5
0
5
10
t [GeV**2]

FIG. 1

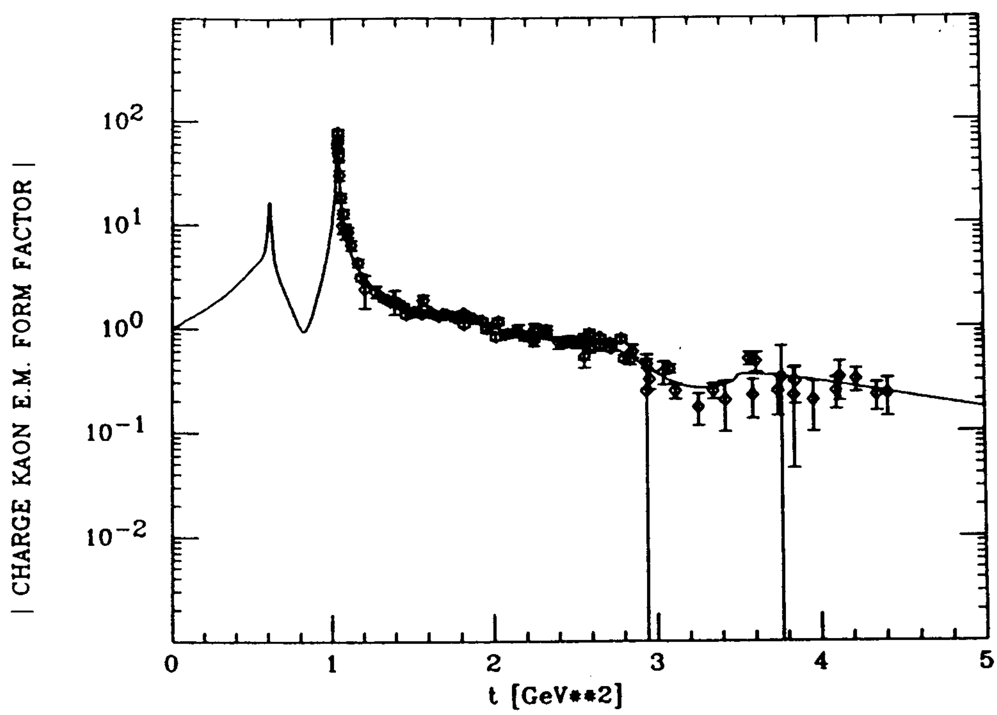
| CHARGE KAON E.M. FORM FACTOR |
10^2
10^1
10^0
10^{-1}
10^{-2}
0
1
2
3
4
5
t [GeV**2]

FIG. 2

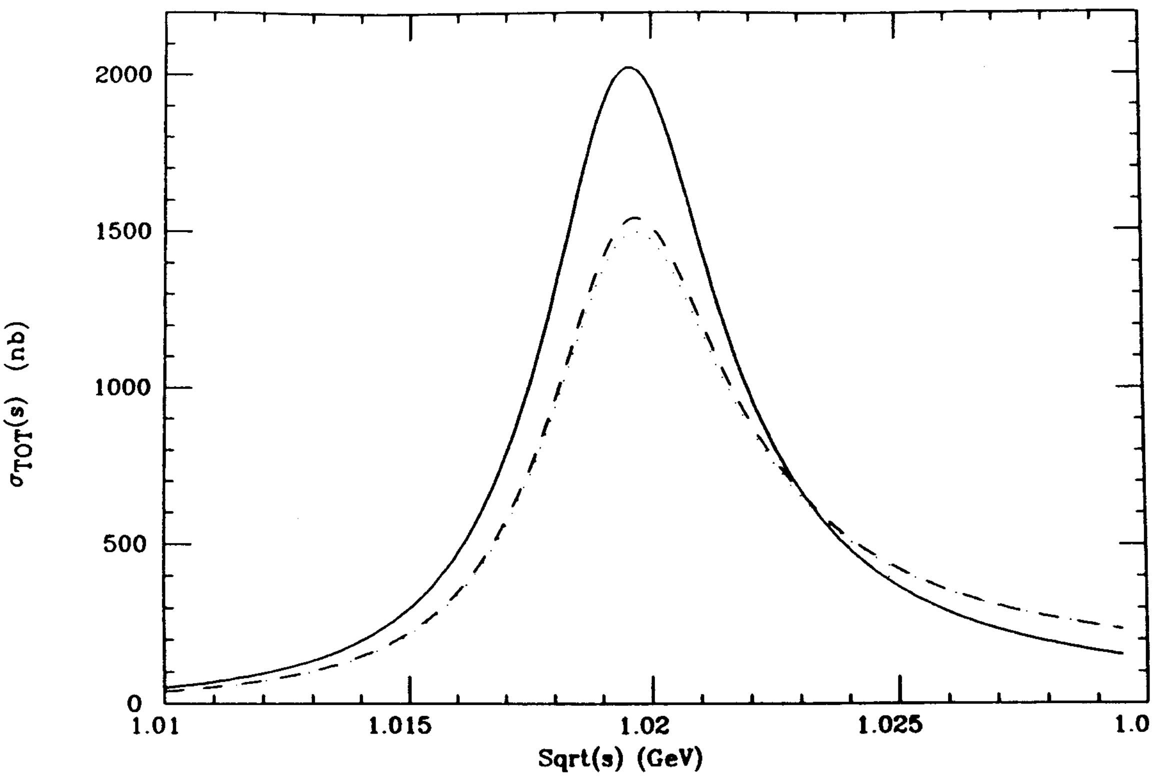

2000
1500
1000
500
0
1.01
1.015
1.02
1.025
1.0
$\sigma_{TOT}(s)$ (nb)
Sqrt(s) (GeV)

FIG. 3

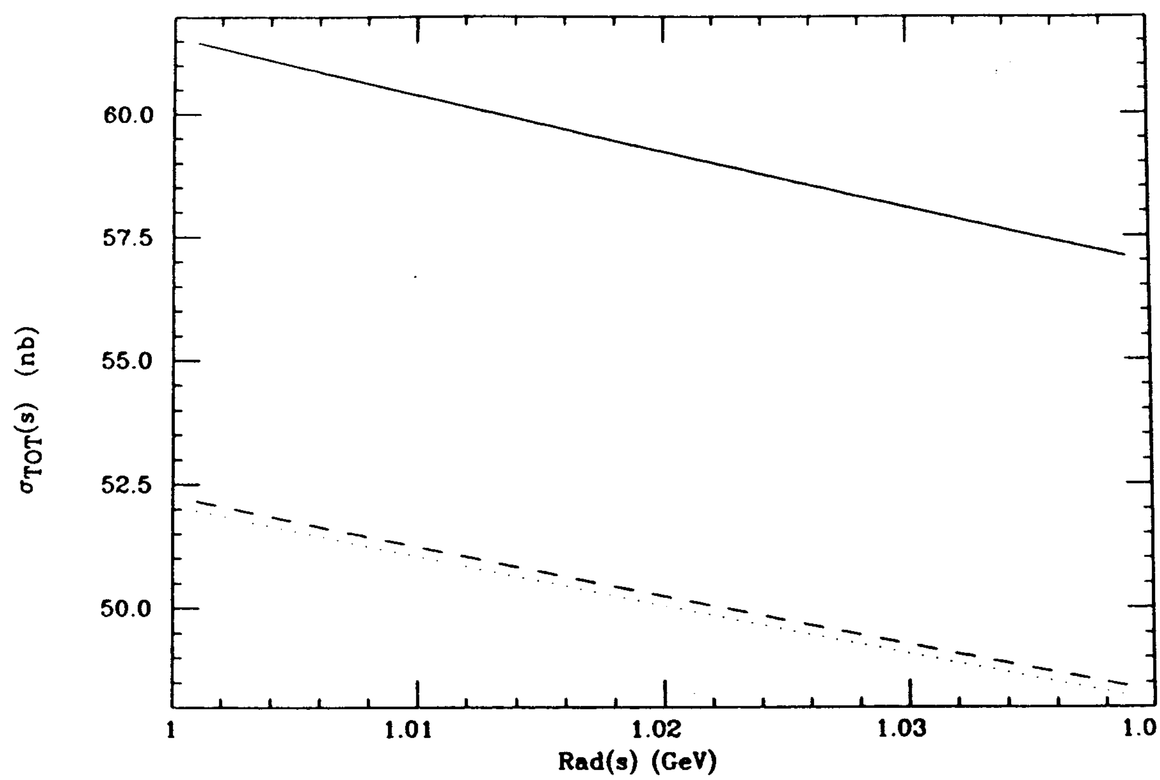

60.0
57.5
55.0
52.5
50.0
1
1.01
1.02
1.03
1.0
$\sigma_{TOT}(s)$ (nb)
Rad(s) (GeV)

FIG. 4a

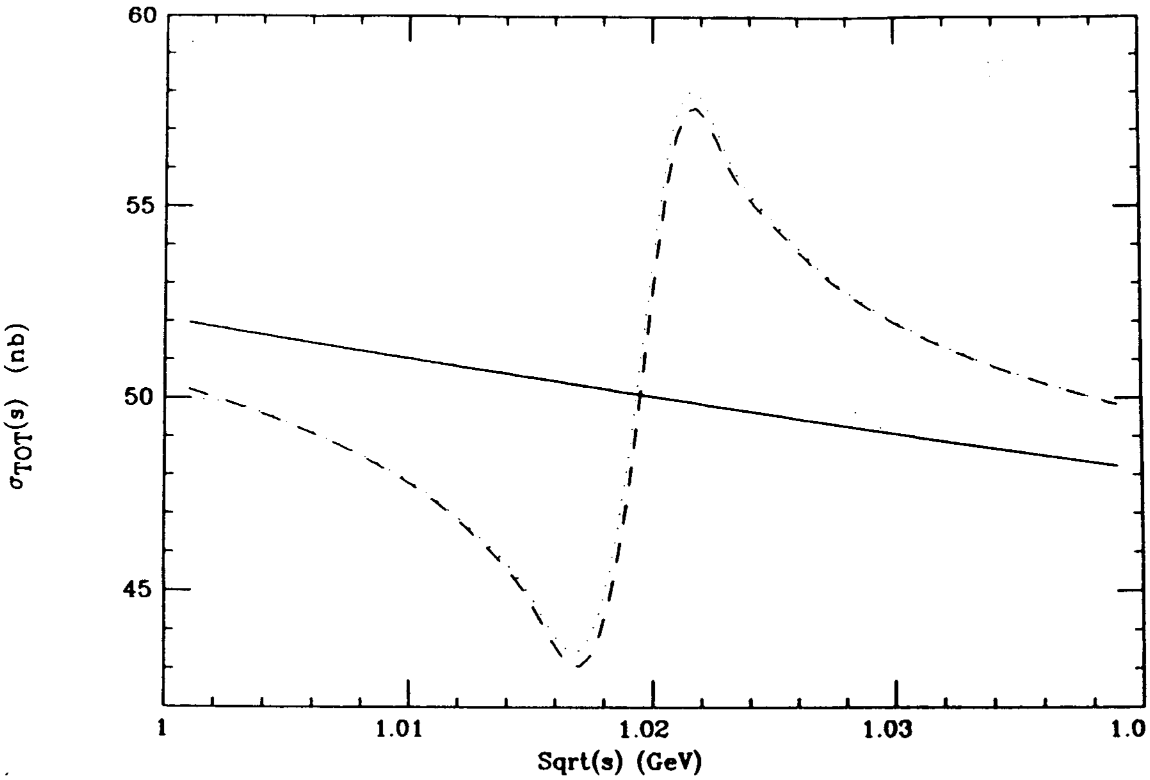
60
55
50
45
$\sigma_{TOT}(s)$ (nb)
1
1.01
1.02
1.03
1.0
Sqrt(s) (GeV)

FIG. 4b

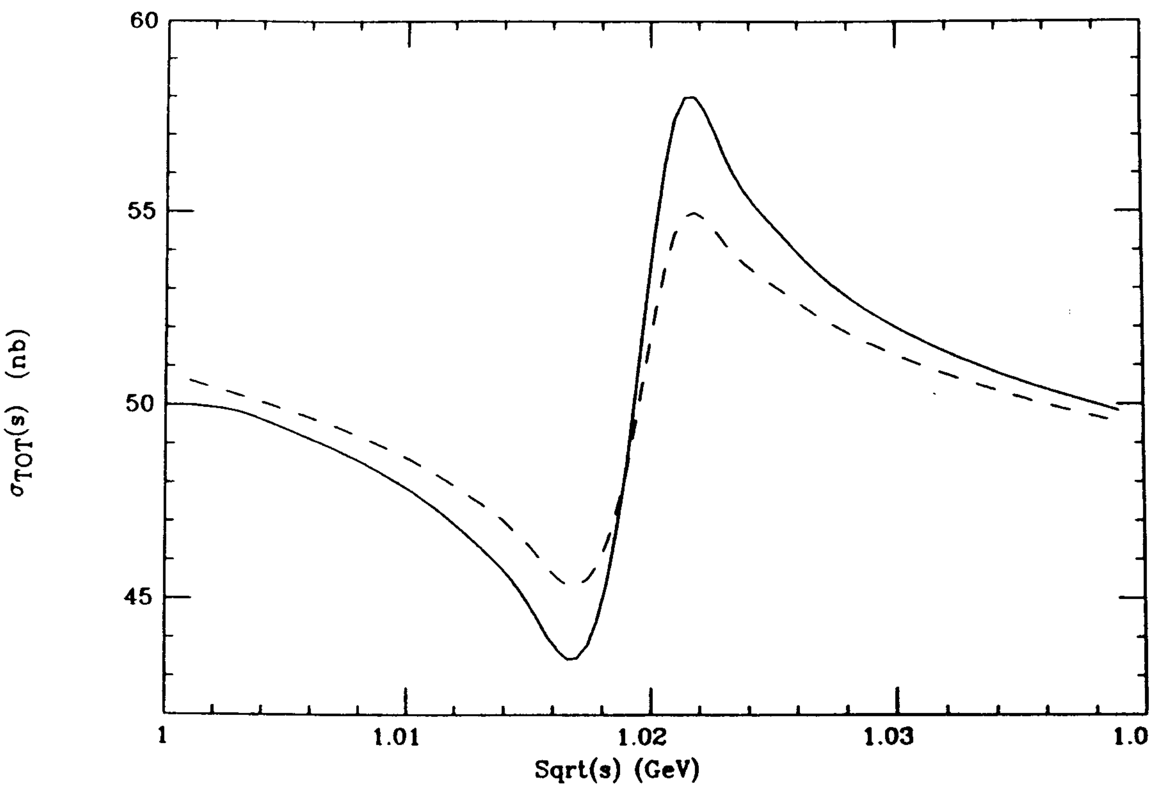
60
55
50
45
$\sigma_{TOT}(s)$ (nb)
1
1.01
1.02
1.03
1.0
Sqrt(s) (GeV)

FIG. 4c

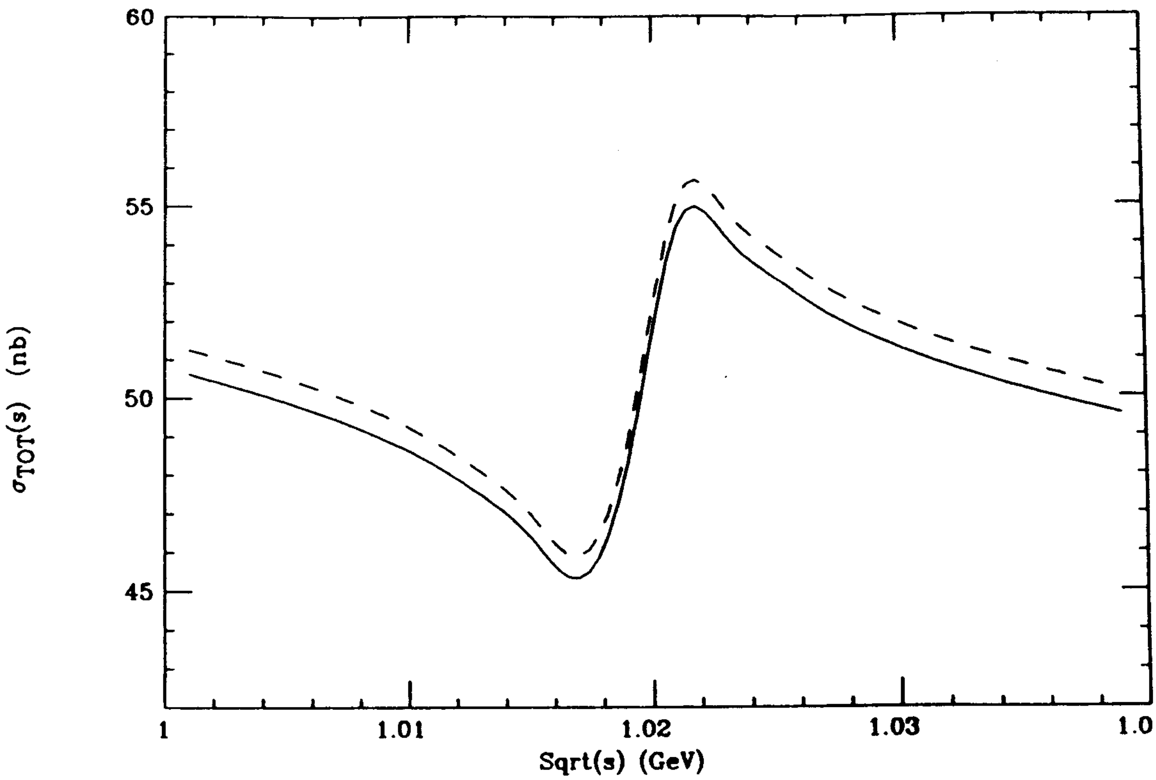
60
55
50
45
$\sigma_{TOT}(s)$ (nb)
1
1.01
1.02
1.03
1.0
Sqrt(s) (GeV)

FIG. 5

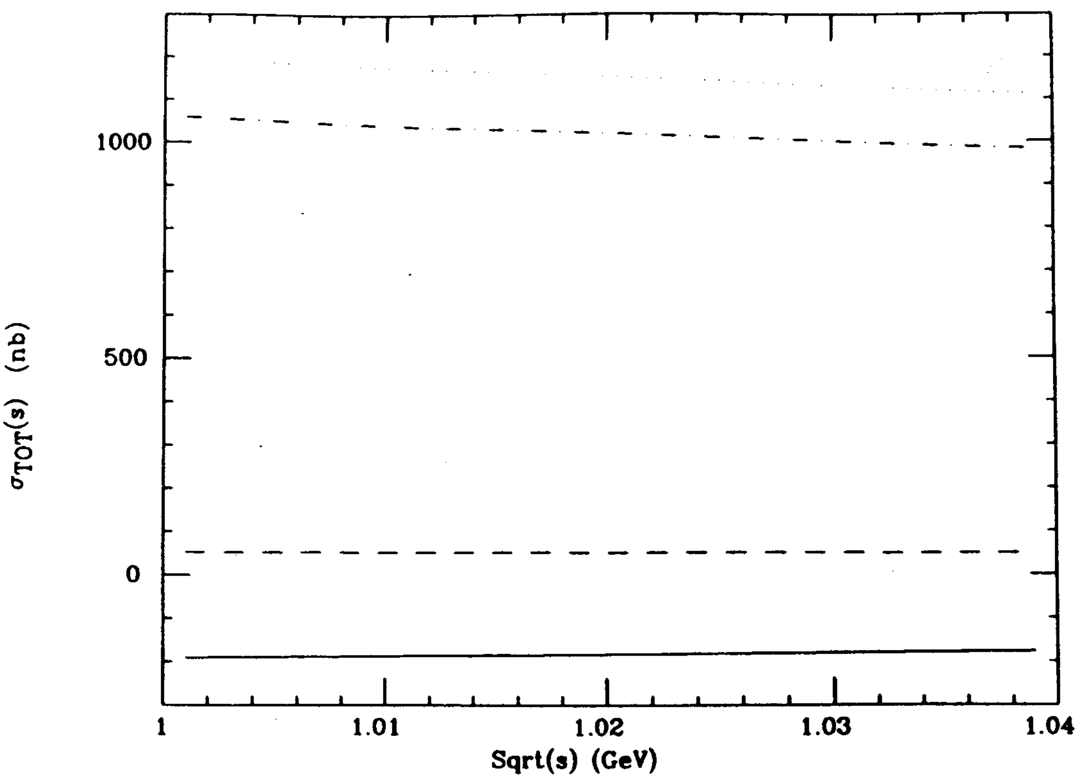
1000
500
0
$\sigma_{TOT}(s)$ (nb)
1
1.01
1.02
1.03
1.04
Sqrt(s) (GeV)

FIG. 6a

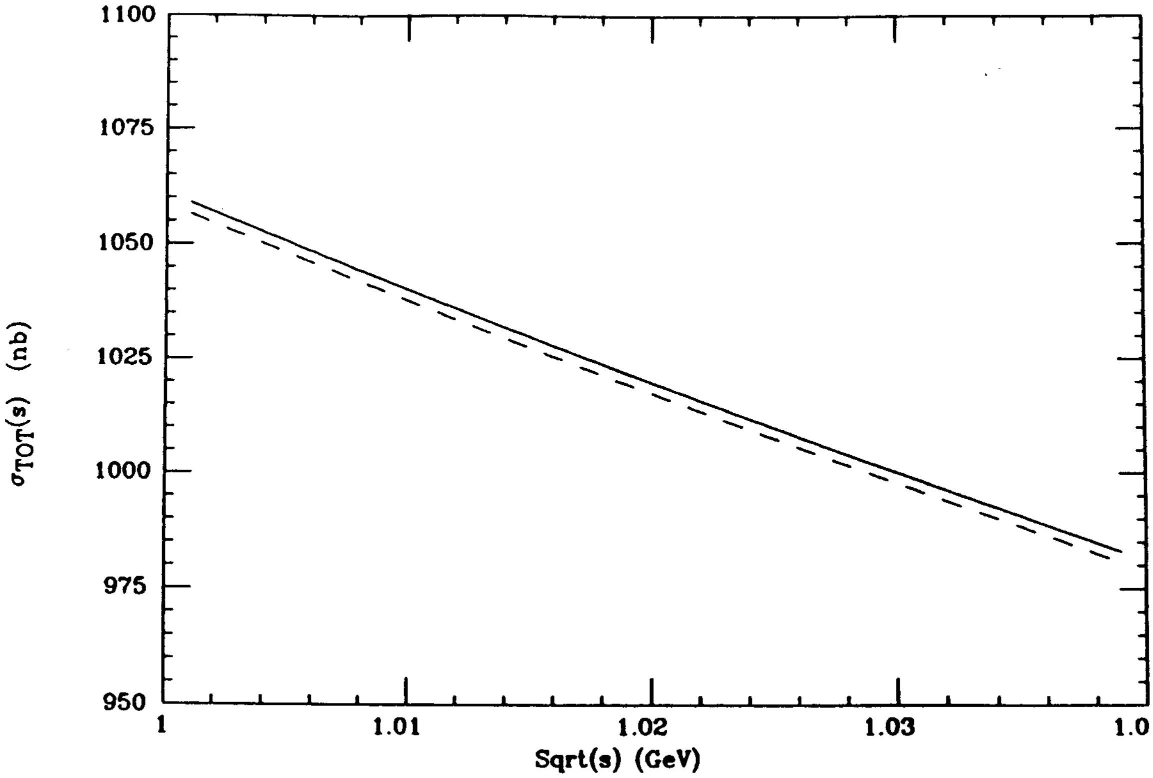
1100
1075
1050
1025
1000
975
950
$\sigma_{TOT}(s)$ (nb)
1
1.01
1.02
1.03
1.0
Sqrt(s) (GeV)

FIG. 6b

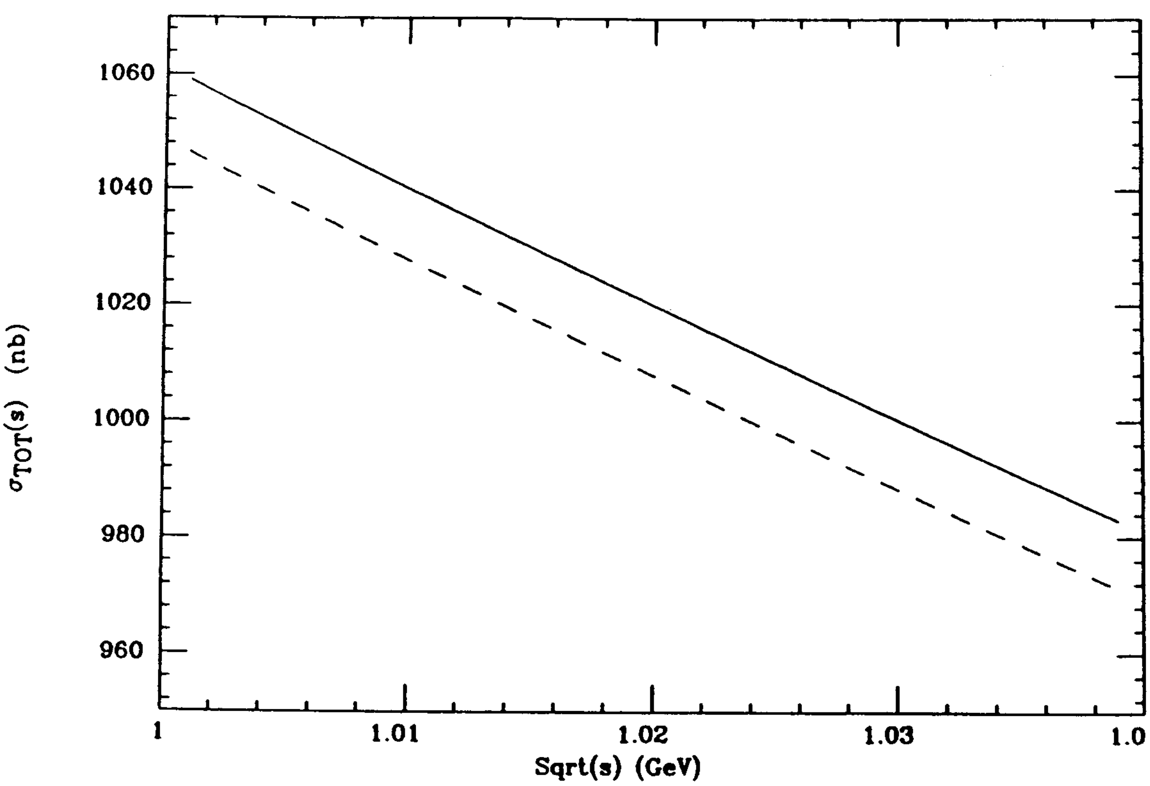
1060
1040
1020
1000
980
960
$\sigma_{TOT}(s)$ (nb)
1
1.01
1.02
1.03
1.0
Sqrt(s) (GeV)

FIG. 6c

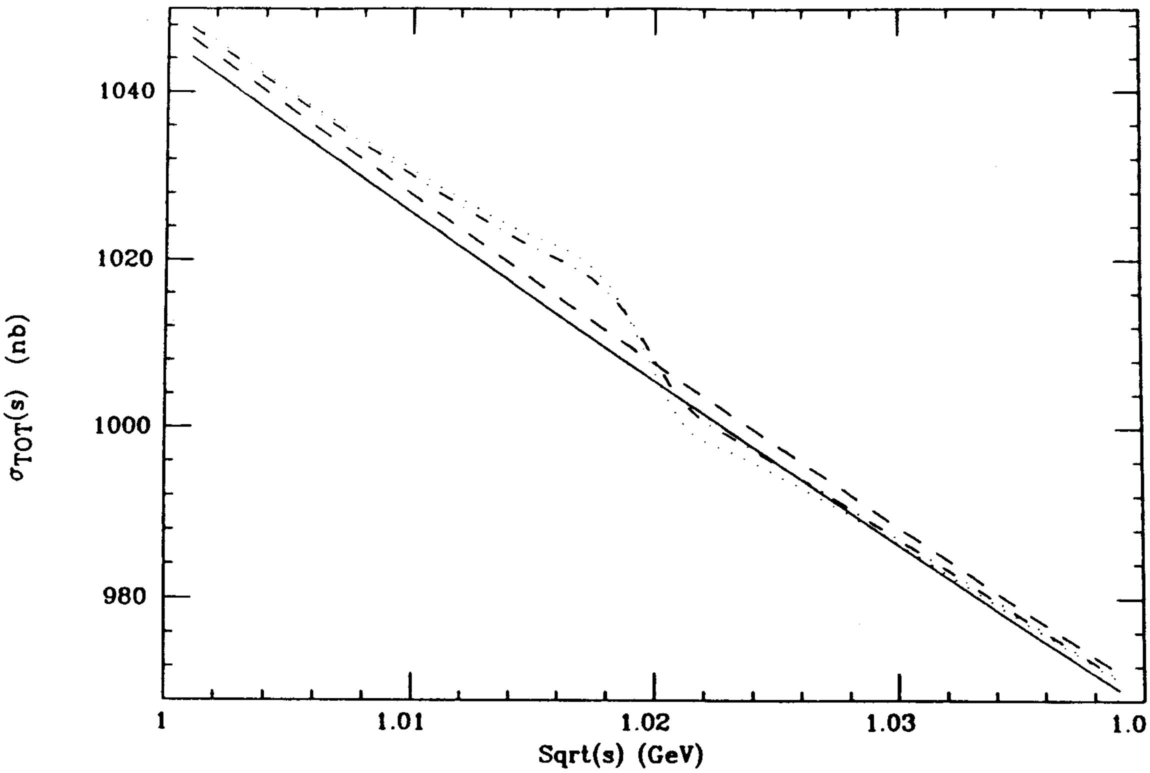

FIG. 7

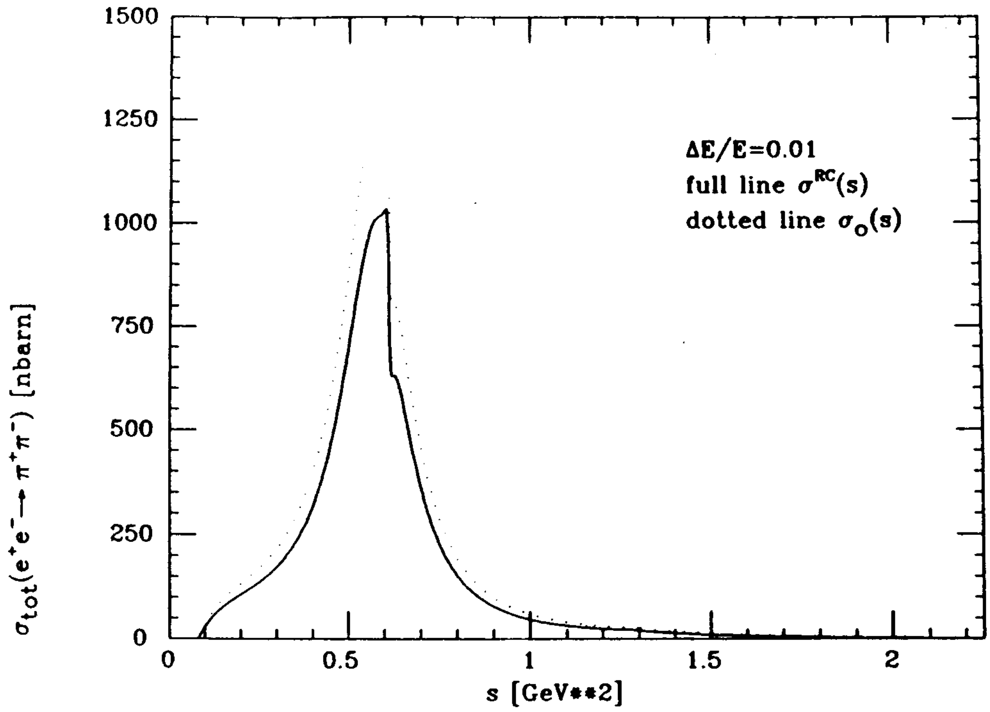
ΔE/E=0.01
full line $\sigma^{RC}(s)$
dotted line $\sigma_0(s)$
$\sigma_{tot}(e^+e^- \longrightarrow \pi^+\pi^-)$ [nbarn]
s [GeV**2]
1500
1250
1000
750
500
250
0
0
0.5
1
1.5
2

FIG. 8a

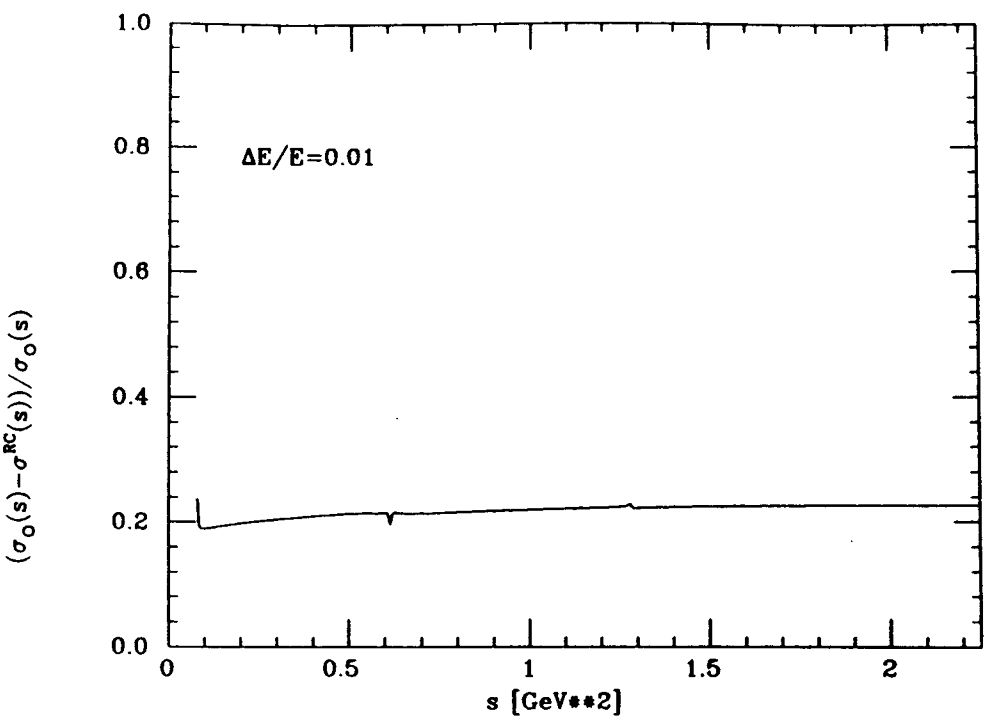
ΔE/E=0.01
$(\sigma_0(s)-\sigma^{RC}(s))/\sigma_0(s)$
s [GeV**2]
1.0
0.8
0.6
0.4
0.2
0.0
0
0.5
1
1.5
2

FIG. 8b

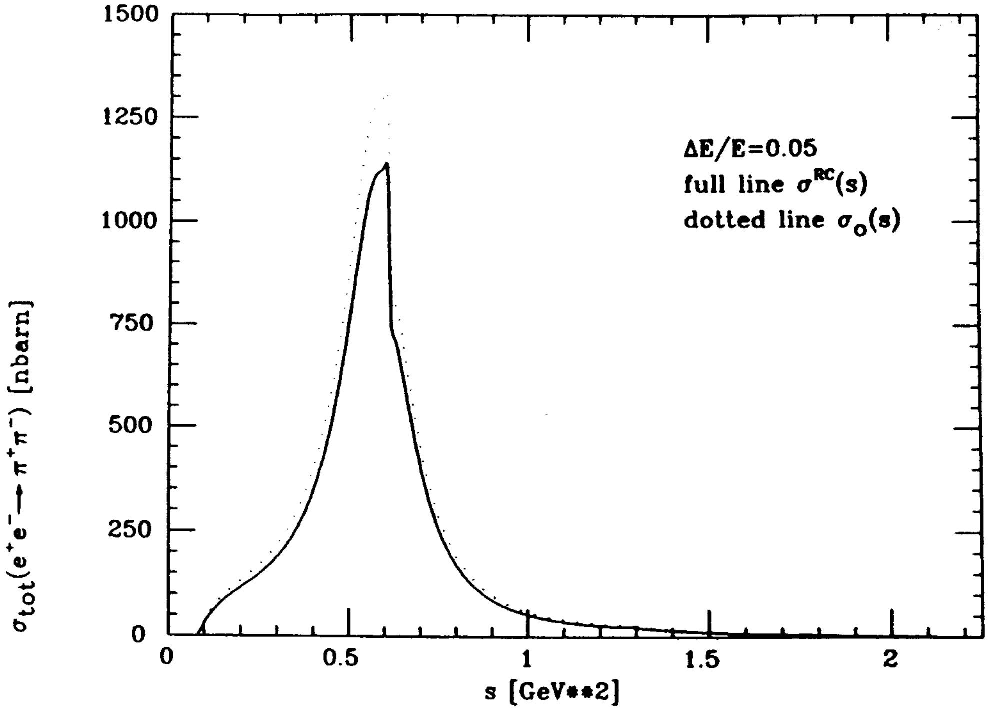
ΔE/E=0.05
full line $\sigma^{RC}(s)$
dotted line $\sigma_0(s)$
$\sigma_{tot}(e^+e^- \to \pi^+\pi^-)$ [nbarn]
s [GeV**2]
1500
1250
1000
750
500
250
0
0
0.5
1
1.5
2

FIG. 9a

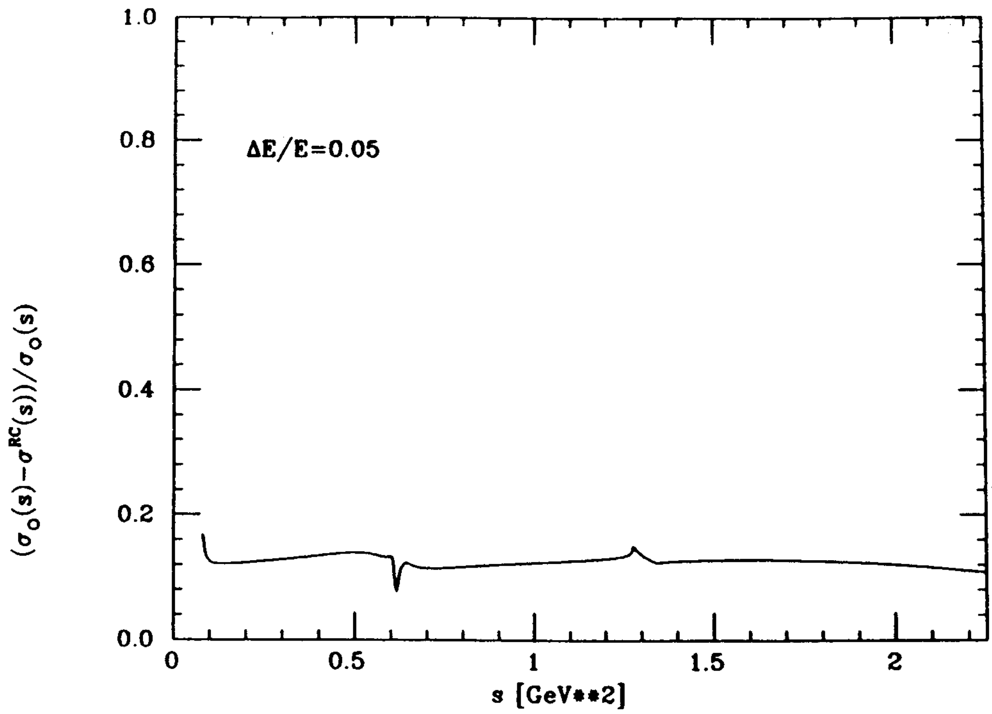
ΔE/E=0.05
$(\sigma_0(s)-\sigma^{RC}(s))/\sigma_0(s)$
s [GeV**2]
1.0
0.8
0.6
0.4
0.2
0.0
0
0.5
1
1.5
2

FIG. 9b

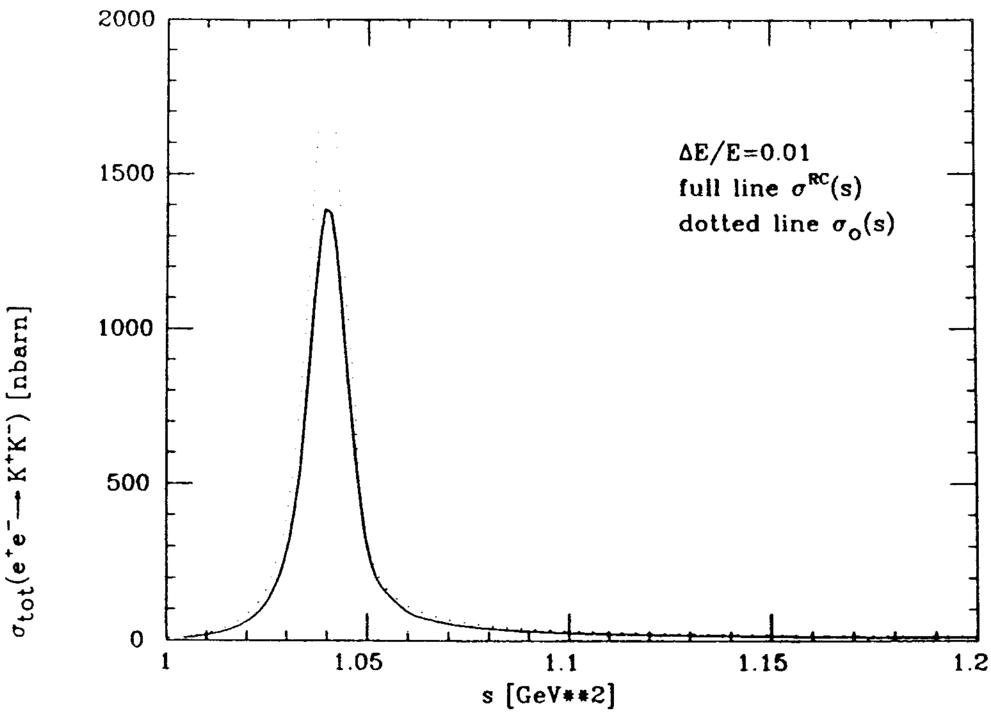

FIG. 10a

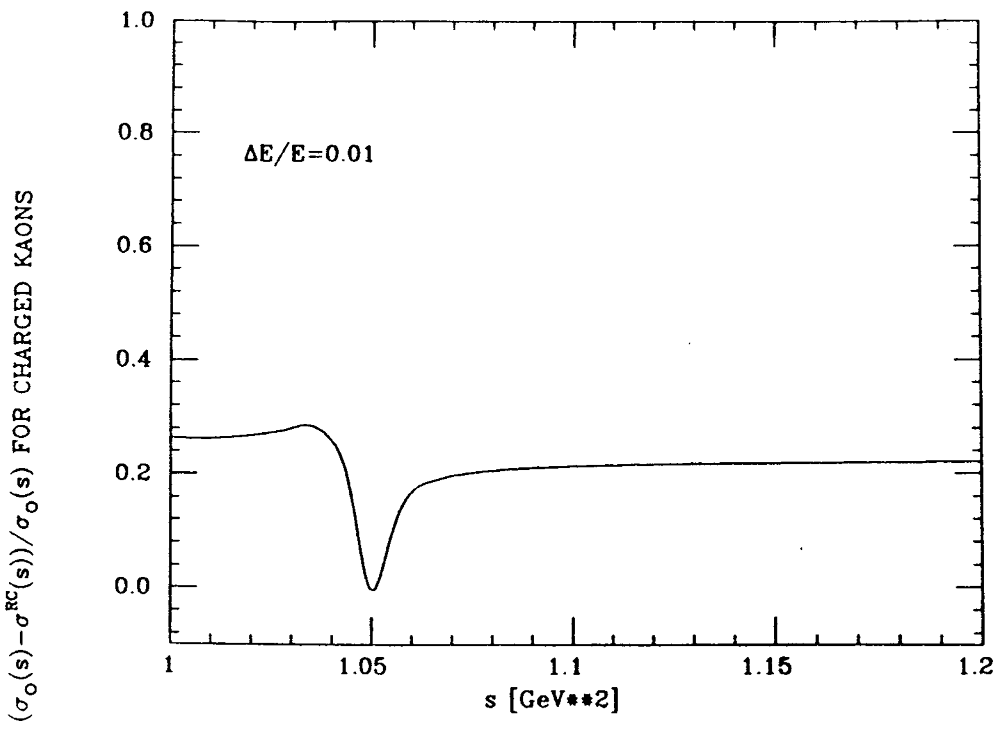

FIG. 10b

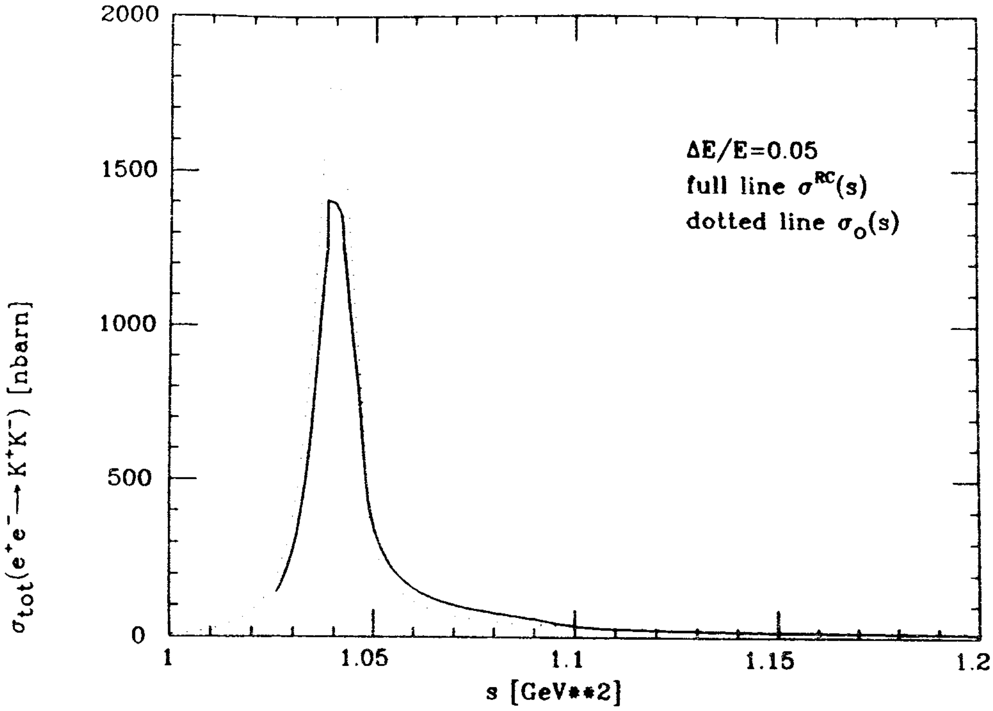

FIG. 11a

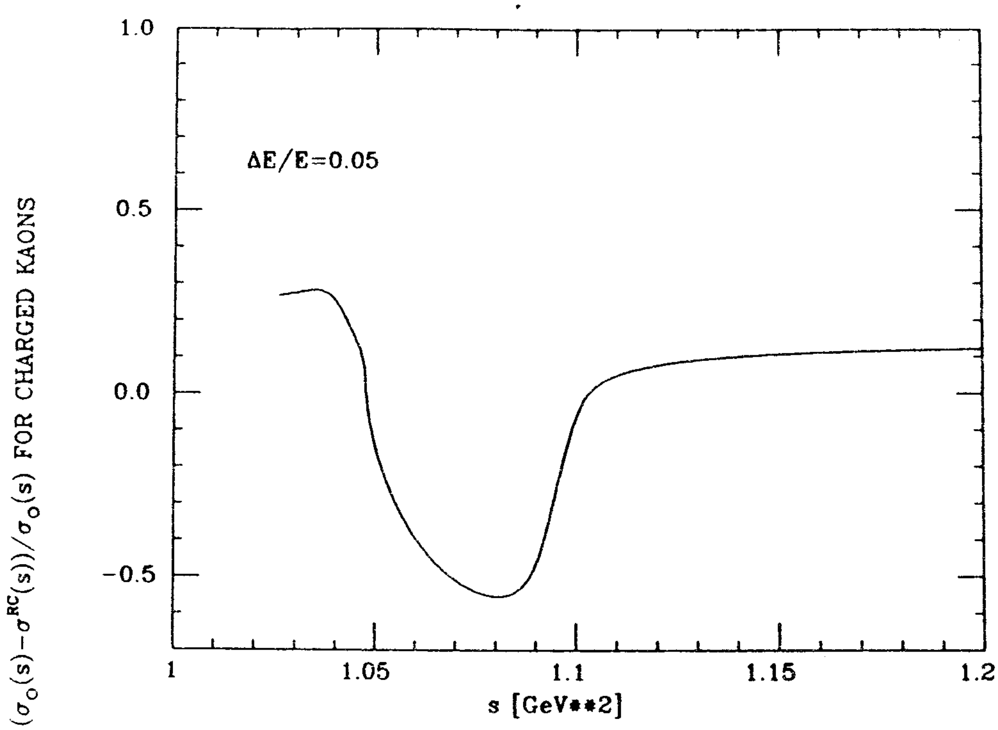

FIG. 11b

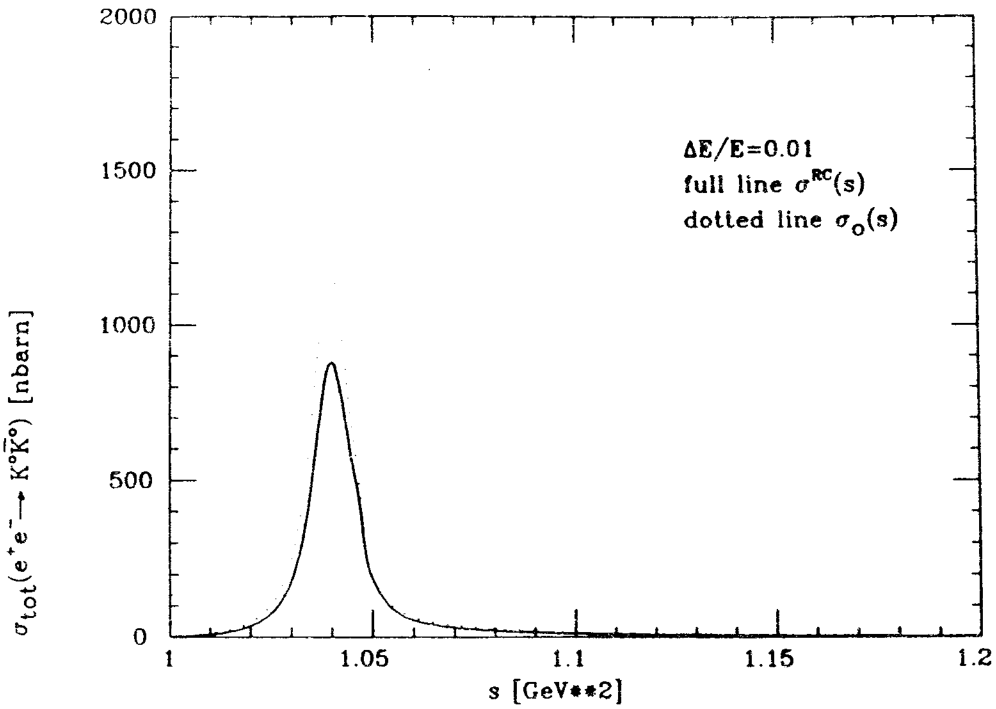

FIG. 12a

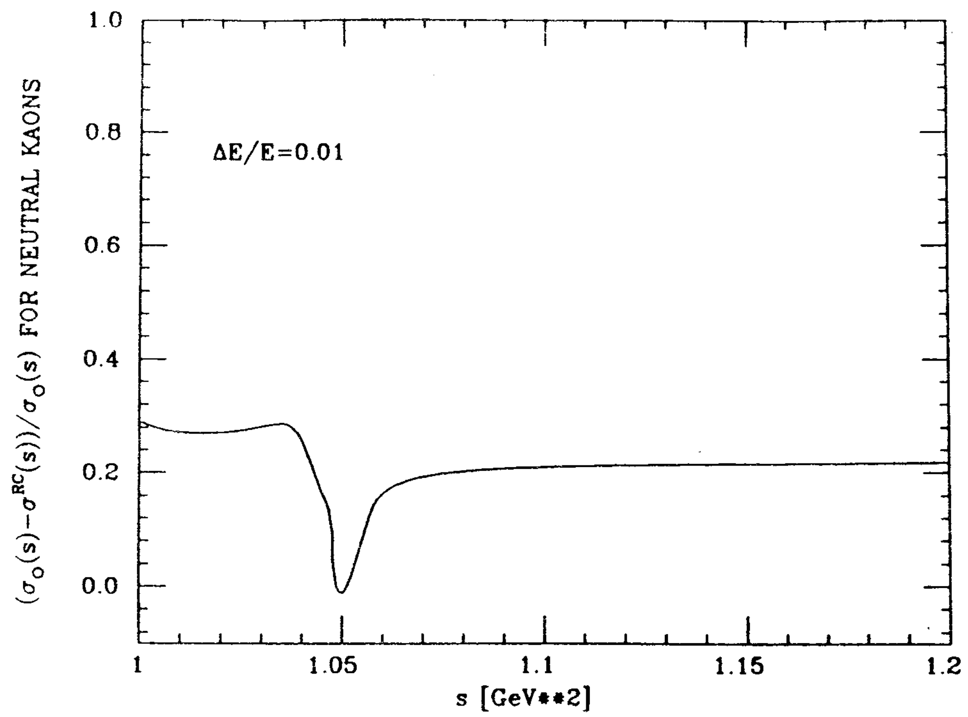

FIG. 12b